Hindawi
International Transactions on Electrical Energy Systems
Volume 2022, Article ID 1860266, 22 pages
https://doi.org/10.1155/2022/1860266

Research Article

Fuzzy-Based EV Charging Station and DVR-Fed Voltage Compensation for a DFIG-Fed Wind Energy System during Grid Faults

R. Uthra,[1] D. Suchitra,[1] Thanikanti Sudhakar Babu ,[2] and Belqasem Aljafari[3]

[1]*Department of Electrical and Electronics Engineering, SRM Institute of Science and Technology, Chennai 603203, India*
[2]*Department of Electrical and Electronics Engineering, Chaitanya Bharathi Institute of Technology, Hyderabad 500075, India*
[3]*Electrical Engineering Department, College of Engineering, Najran University, Najran 11001, Saudi Arabia*

Correspondence should be addressed to Thanikanti Sudhakar Babu; sudhakarbabu66@gmail.com

Received 30 December 2021; Revised 17 May 2022; Accepted 23 May 2022; Published 14 July 2022

Academic Editor: Sobhy Abdelkader

In recent years, it can be seen that more and more wind energy systems are integrated to focus on developing a more reliable energy system. A doubly-fed induction generator is the most employed machine in wind energy systems having the advantages of variable speed operation, improved power quality, and high energy capture. In a wind energy conversion system (WECS), the generator's capability to remain connected during short electric faults resulting in voltage sag is known as fault ride through (FRT). Over the last few years, electric vehicles have been providing a remarkable solution for many sustainability issues such as global warming, depletion of fossil fuel reserves, and emission of greenhouse gas that needs attention to detail. A voltage compensation using Dynamic Voltage Restorer and Electric Vehicle charging station both employing a fuzzy controller is proposed in this paper for sustaining FRT capability. The variation in the stator voltage is tracked and utilized to inject the necessary shortfall of voltage in the system via DVR or EV charging station for the intensity of the created voltage sag. Vehicle-to-grid unit of the electric vehicle charging station comes into action when voltage sag intensity is 0.9 p.u. to 0.51 p.u. Value of the nominal voltage and the DVR takes over when voltage sag falls between 0.5 p.u. and 0.2 p.u. Consequently, this voltage compensation regulates the other relative parameters like DC link voltage and active power and retains them within the permissible limits during the fault.

1. Introduction

With increasing awareness with respect to the depletion of natural energy resources, the shift toward renewable energy is the main focus in recent years. In this regard, the changes in the transportation industry have become inevitable, enabling the transition to electric vehicles. Till 2019, approximately 4.8 million of battery electric vehicles (BEVs) were operative globally, and about 1.5 million of new BEVs were introduced throughout the world [1]. Electric vehicles play a very imperative role in sustaining a zero-emission, healthy environment. Thereupon, more and more EV charging stations are being developed to cater to the arising needs for electric vehicles globally. As of March 2021, there are 1800 EV charging stations in India [2]. With this increasing penetration of electric vehicles into the global market, many EV charging stations are being set up to cater to the needs of the EV. An EV charging station can also be utilized as an adaptable load connected to the grid to normalize the fluctuation of voltage during power generation. In this regard, the main idea of this paper is to fuse an EV charging station with a grid integrated wind energy system.

The development of modern wind energy conversion systems has been one of the primary sources of energy since 1970 and in recent years WECS has seen a vast penetration in the energy market. In governing the WECS, an important requisite called grid codes was amended in the last decades to measure up to the technicalities needed for a wind farm. These grid codes are divided into two types namely static and dynamic stipulations. Steady-state performance and power

flow analysis fall under static stipulations, and the response of the generator during faults like operating voltage range, frequency, and FRT capability comes under dynamic stipulations. Among the grid codes, FRT capability is the most challenging one. FRT identifies the capability of a WECS to continue being connected to the grid, for a short duration of time when a fault occurs at the grid. FRT basically warrants any fault which can be usually rectified, and evidently there is absolutely no loss in wind power being generated. Figure 1 indicates the FRT characteristics based on per grid codes followed in India [3]. In the characteristics, V_f denotes 15% of the nominal value of the voltage, and V_{pf} denotes 80% of the nominal value of the voltage. Hence, the wind turbine stays connected with the system within the duration of "T" seconds. This necessitates FRT protection and voltage compensation to recover the voltage within this specified time limit. The wind turbine generators will continue to provide active power proportional to the grid voltage instantly after the fault is cleared.

Variable speed generators (VSGs) are being increasingly used in WECS as they provide excellent frequency support and active and reactive power supply. Among various types of VSGs available, the Doubly Fed Induction Generator proves to be a major point of interest due to its several advantages. Some DFIGs have independent control concerning active and reactive power, have relatively less mechanical stress, and can be directly connected to the grid. The main issue about DFIG is that it is directly connected to the grid and hence any fault occurring at the PCC makes it very sensitive creating voltage sags [4–7]. Therefore, as per the grid codes, the FRT capability should be effectively carried out, thereby providing voltage compensation depending on the intensity of the voltage sag. Thus, DFIG-based WECS needs auxiliary support for voltage compensation during fault.

In grid integrated system, fault diagnosis has attracted growing attention to minimize system downtime and avert severe damage to the power system. As a result, Yang et al. provided a current state-of-the-art assessment on wind converter fault diagnosis of wind energy systems including both model-based and pattern-based techniques [8]. The primary requirement in fault diagnosis is to design two separate control loops, one on the rotor side and the other on the grid side. Many researchers in the literature have explored various control strategies in this regard. Two independent controls, namely rotor side control (RSC) and grid side control (GSC), have been analyzed in detail [9–12]. In all the above papers concerning fault diagnosis, various control circuits involving the control of rotor and grid parameters have been discussed. Out of all these methods, vector or field-oriented control is used largely as it provides competent regulation of rotor and grid parameters.

Sardar Kamil et al. [13] reviewed the several control strategies for maintaining the low voltage ride through (LVRT) capability of grid-feeding converters, with their benefits and drawbacks, thereby presenting a comparative listing of various current control loops where vector control is chosen as the primary control with various rotor parameters as reference. In [14], stator flux orientation and

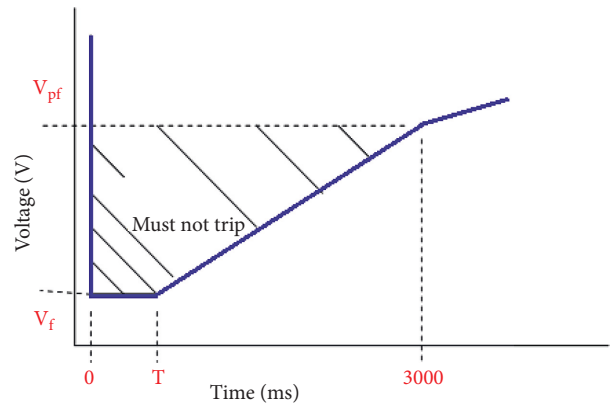

Figure 1: FRT characteristics.

Lyapunov theory are proposed as an LVRT solution with an enhanced control technique of stator powers exchanged between the DFIG and the grid. Geng et al. developed control strategies with grid side converters (GSCs) for unsymmetrical faults in grid integrated wind systems [15, 16]. In all the above-said literature, vector control was taken as the fundamental control scheme with different variables as reference. Hence, considering all this survey, a vector control scheme with reactive power and DC link voltage as references have been adopted for the grid, along with rotor control in this paper. Even with an appropriate control strategy, the voltage sag developed due to fault is not compensated. Hence, it becomes necessary to identify enhancement solutions to achieve FRT.

Appropriate solutions for FRT should be provided by protecting, compensating, and regulating the voltage during fault at the grid. These solutions can be provided as an external retrofit or internal control circuitry. External retrofit refers to auxiliary power electronic devices to protect the system and compensate for the voltage in the event of a fault. Flexible AC Transmission System (FACTS) devices have been used to provide supplementary support for a long time. FACTS devices based on power injection are used to achieve FRT and also help to uphold the transient stability of the system. But these devices are added additionally to the grid integrated system with their own control unit which increases the total complexity of the system. The main classification of auxiliary devices for FRT capability is depicted in Figure 2. Amongst all the protection methods, the crowbar protection proves to be the simplest and most productive circuit [17]. Noureldeen et al. discussed intelligent protection techniques with a crowbar to attain FRT in DFIG-based WECS [18, 19]. As the main focus of this paper is voltage compensation during the fault, therefore the crowbar protection which has already been established as an effective technique is included in the proposed system with a fundamental crowbar circuit.

The voltage imbalance caused by the fault can be evened out using auxiliary support devices. Some of the largely used support devices are shown in Figure 2. The compensation using Static Synchronous Compensator (STATCOM) supercapacitor system at the PCC in DFIG fed wind system is detailed in [20]. STATCOM is primarily a voltage source

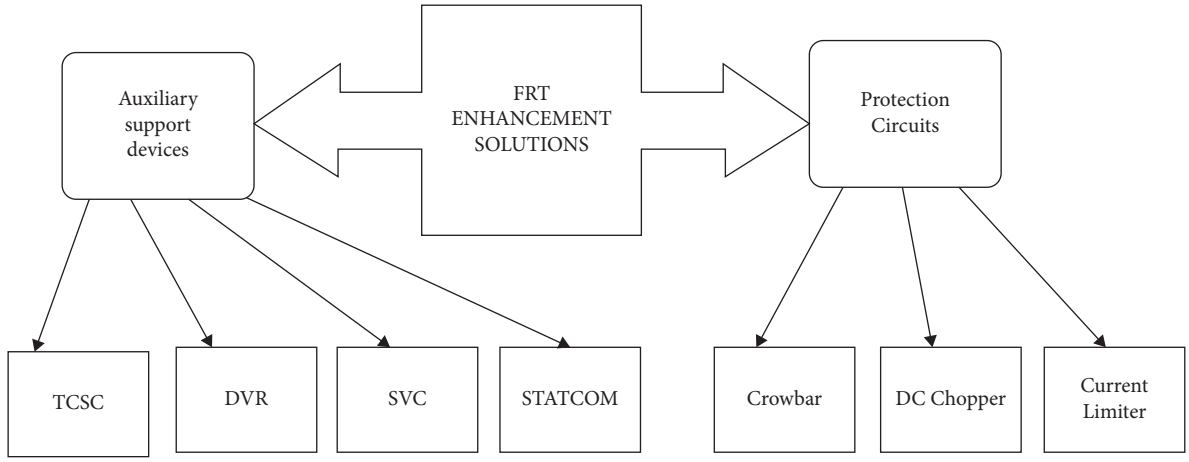

Figure 2: FRT enhancement methods.

inverter which is fed from a DC capacitor. Hence, during the event of fault voltage recovery, STATCOM produces a decelerating torque in the generator. Hiremath et al. [21] presented the latest techniques of LVRT for different wind generators using different converter controllers. Many control schemes were discussed in detail and the merits and demerits of different schemes were highlighted. Many of the reviewed control schemes had taken vector control as the basis with different controlling parameters to regulate active and reactive power. FRT capability using Static Var Compensator (SVC) is addressed in [22]. SVC is a shunt-connected FACTS device that improves voltage stability and regulation. The shunt-connected devices are capable of providing smooth and swift steady-state as well as transient voltage control at PCC. But unstable voltage oscillations occur in shunt compensation. Also, this type of compensation is not very effective in high voltage fault conditions, unlike series connections.

DVR which is a device connected in series is found to give the best performance and stabilizes the wind generator system very effectively. The biggest advantage of DVR voltage compensation is that during steady-state conditions, the DVR stays idle and only during the duration of fault, depending on the value of voltage, sag appropriate voltage is injected. DVR has been implemented with dual voltage controllers in [23]. This makes the circuit sluggish and thus it takes a longer time for the restoration of voltage. DVR with a conventional PI controller proved to give a better response than the dual voltage controllers [24, 25]. But this paper does not include error tracking in voltage for various faults. He et al. [26] proposed an LVRT scheme for a grid integrated wind/PV hybrid system. This paper has presented an active output control by taking DC link voltage as reference for vector control to provide stable active and reactive power during faults thereby improving the dynamic response of the system. In [27], DVR is operated with a fuzzy controller to regulate the injecting value of voltage during a fault, based on the voltage sag. This yielded a fairly good control of DVR, but it was not integrated with any power system but intercepted individually. Hence, in the proposed technique, a fuzzy controlled DVR for voltage compensation as a secondary compensation device during fault is integrated with a grid-connected WECS.

The number of EV charging stations that are allotted incentives in various states in India, as of January 2020, is shown in Table 1 [28]. With the current and upcoming trend of EV charging stations, it can be used as a compensation device in larger rating generation systems rather than introducing an additional supplement device. Based on the demand from the grid and the site of charging stations, EVs collaborate and discharge their energy to the grid for a certain duration of time, thereby adjusting the voltage and frequency of the electric power in the grid. The batteries themselves in EV charging stations are powered using independent renewable energy sources and thus completely making the system sustainable in all aspects. In this regard, an idea of an EV charging station available nearest to the renewable power generation system has been slated as a primary compensation in this paper. On reviewing the literature concerning this type of compensation, various papers support the credibility of this idea.

In a hybrid AC/DC system, a coordinative control in charging hybrid electric vehicles has been introduced [29]. A vehicle-to-grid (V2G) unit is explored, where a grid-connected electric vehicle charging station supplies a distributed system based on the deviation in the frequency at the plug-in terminal, depending on the imbalance in the power grid [30]. Hence, this paper mainly contemplates frequency deviation at PCC rather than voltage variation during faults. Mohammad et al. [31] articulated that EVs can operate as a supplementary unit, to minimize the challenges related to renewable energy systems and thus provide ancillary services to the grid, in regulating voltage and frequency. But the DFIG-based wind system is more proactive concerning energy management. Hence, applying the above-said compensation to a DFIG-based system will prove to be more effective in managing power during faults.

Literature [32, 33] focused on the contemporary modeling of grid-connected PV systems tied to EV charging stations. This idea can be extended to wind energy systems

Table 1: EV chargers sanctioned under FAME.

S. No.	State	Allotment for EV charging stations
1)	Maharashtra	317
2)	Andhra Pradesh	266
3)	Tamil Nadu	256
4)	Gujarat	228
5)	Uttar Pradesh	207
6)	Rajasthan	205
7)	Karnataka	172
8)	Madhya Pradesh	159
9)	West Bengal	141
10)	Telangana	138
11)	Kerala	131
12)	Delhi	72
13)	Chandigarh	70
14)	Haryana	50
15)	Meghalaya	40
16)	Bihar	37
17)	Sikkim	29
18)	Jammu and Kashmir	25
19)	Chhattisgarh	25
20)	Assam	20
21)	Odisha	18
22)	Uttarakhand	10
23)	Puducherry	10
24)	Himachal Pradesh	10

integrated with EV charging stations for voltage compensation. In all the above-discussed V2G units, the battery charging units are regulated with a PI controller.

Taking all the literature review into consideration, it can be seen that the voltage compensation during fault has been carried out with only one primary device. Table 2 summarizes the benefits of various sectors on integrating electric vehicles into the grid [25]. This paper proposes a technique that involves a primary as well as a secondary compensation using a V2G unit and a DVR. The EV charging station is becoming a needful one with more and more electric vehicles being introduced as a form of green energy unit. Hence utilizing the battery unit available in the charging station as a support device in addition to a secondary unit of DVR is the main novelty presented in the proposed system. In the proposed WECS, a V2G unit with a fuzzy controlled battery unit acts as a primary source of compensation device providing precise control during charging and discharging of the batteries, and a fuzzy controlled DVR is used as a secondary compensating device. A fuzzy-based control provides clear compensation and control even in the vague input conditions as well as transient conditions.

The significant contribution of this paper is that the two support devices will operate based on the voltage sag intensity.

(i) The feasibility of using an electric vehicle charging station as an auxiliary support device during fault to achieve FRT capability has been analyzed and successfully achieved.

(ii) A venture has been made to devise a strategy in using DVR and EV chargers as primary and secondary compensation devices depending on the intensity of the fault in grid integrated wind systems.

(iii) The EV charging station has to charge electric vehicles; hence, the proposed system has been designed in such a way that when the intensity of voltage sag is less (0.9 p.u. to 0.51 p.u.), the EV charging station supplies voltage to the grid to restore the original voltage.

(iv) As for the fault with higher intensity voltage sag (0.5 p.u. to 0.2 p.u.), the secondary device DVR takes over to provide voltage compensation by tracking the deficit voltage.

(v) Both the compensating units of the EV charging station and DVR are regulated with a fuzzy controller and can provide accurate compensation with a wide range of operating conditions, unlike PI controllers.

The course of this paper is organized as follows: Section 2 outlines the modeling and control of WECS. The design and control of DVR and EV charging stations are discussed in Sections 3 and 4 respectively. Section 5 illustrates the different modes of operation of the complete system which is followed by the discussion of simulation results in Section 6. The conclusion of the paper is proffered in Section 7.

2. Wind Energy Conversion System

Wind turbines basically convert kinetic energy to electrical energy as indicated in Figure 3. Maximum power is extracted from the wind turbine using an MPPT controller. The DFIG generates electrical output. Operating a wind system, there involves two controllers namely RSC and GSC.

RSC and GSC have connected with a capacitor called a DC link capacitor and the voltage that appears across this capacitor is denoted as V_{DC}. The primary role of RSC is to control and regulate the rotor parameters. Similarly, GSC does the job of sustaining the DC link voltage to a constant value. The output from the grid side inverter is fed to the grid which in turn feeds the stator of the DFIG.

2.1. Modeling of DFIG. DFIG parameters are defined in dq reference frame for both stator and rotor [34, 35]. The grid voltage is linked with the DFIG stator. The DFIG equivalent circuit is depicted in Figure 4 with all the voltage and current parameters represented in dq reference frame.

Descriptive equations of DFIG are [19]

$$\begin{aligned} V_{ds} &= R_s i_{ds} + \frac{\mathrm{d}\lambda_{ds}}{\mathrm{d}t} - \omega_e \lambda_{qs}, \\ V_{qs} &= R_s i_{qs} + \frac{\mathrm{d}\lambda_{qs}}{\mathrm{d}t} - \omega_{\mathrm{e}} \lambda_{\mathrm{ds}}, \\ V_{dr} &= R_r i_{dr} + \frac{\mathrm{d}\lambda_{dr}}{\mathrm{d}t} - (\omega_{e-} \omega_r) \lambda_{qs}, \\ V_{qr} &= R_r i_{qr} + \frac{\mathrm{d}\lambda_{qr}}{\mathrm{d}t} - (\omega_{e-} \omega_r) \lambda_{qs}, \end{aligned} \tag{1}$$

where V_{ds}, V_{qs} = dq axes stator voltages, V_{dr}, V_{qr} = dq axes rotor voltages, i_{ds}, i_{qs} = dq axes stator currents, i_{dr}, i_{qr} = dq axes rotor currents, λ_{ds}, λ_{qs} = stator flux linkages of dq axes,

Table 2: Electric vehicle grid integration benefits.

S. No.	Sectors	Benefits
1.	Distribution system	(i) Delay of distribution capacity upgrades (ii) Better assimilation of renewables and reduction in backflow on the distribution system in high solar penetration areas (iii) Voltage support and resiliency services (reliability services)
2.	Transmission system	(i) Delay of transmission capacity expansion (ii) Better integration of renewables (iii) Primary frequency response and voltage support (iv) Operational efficiency and black-start services
3.	Wholesale market	(i) Primary and secondary regulation of frequency (response) (ii) Reactive power support and management of energy imbalances
4.	Compliance	(i) Utilities/consumers: achievement of regulatory requirements and/or renewable energy targets (ii) Cities/states: achievement of renewable energy targets
5.	Societal and environment	(i) Reduction of power system/transport sector's carbon footprint (ii) Reduction of criteria air pollutants and air toxics (iii) Creation of economic opportunities (iv) Generation of employment and upskilling opportunities

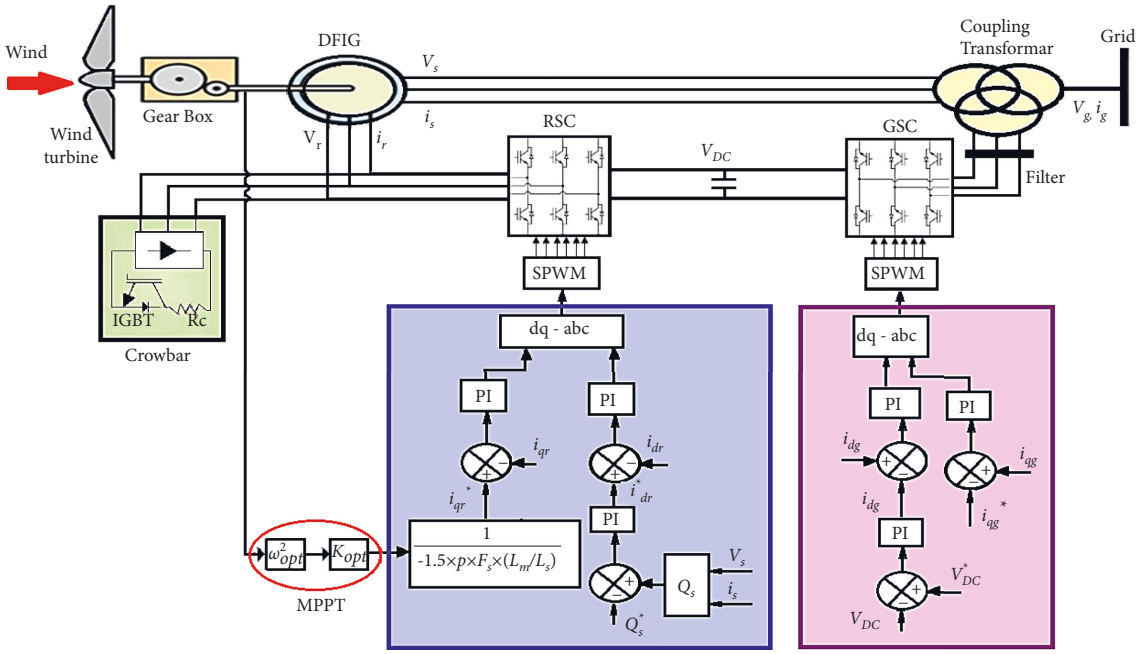

Figure 3: Wind energy conversion system with RSC and GSC.

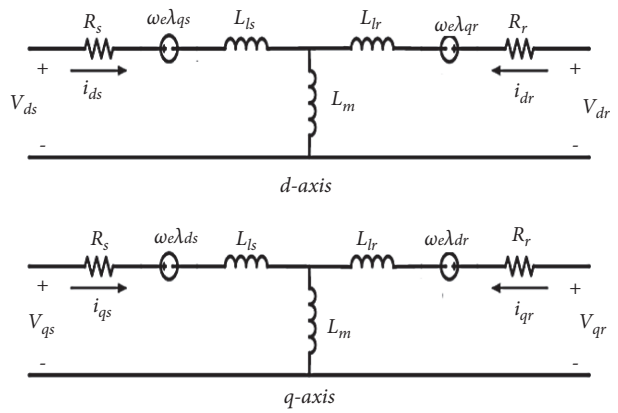

Figure 4: Doubly fed induction generator equivalent circuit.

$\lambda_{dr}, \lambda_{qr}$ = rotor flux linkages of dq axes, and R_s, R_r = resistances of stator and rotor.

Active and reactive powers are

$$P_s = \frac{3}{2}\left(V_{qs}i_{qs} + V_{ds}i_{ds}\right),$$
$$Q_s = \frac{3}{2}\left(V_{qs}i_{qs} - V_{ds}i_{ds}\right). \quad (2)$$

2.2. Rotor Side Converter. RSC as shown in Figure 5 is made up of power converters with their own control unit. The active and reactive powers are controlled by establishing minimum power loss during power conversion and are achieved through a vector control scheme. In this scheme, the measured three-phase rotor currents are converted to their corresponding dq axes equivalents. The d-axis parameter controls the reactive power and the q-axis the active power. The current in d-axis (i_d) and the current in q-axis (i_q) are obtained and are then fed to the PI controllers to obtain the voltage reference values which are fed to a pulse width modulated converter to generate converter pulses.

2.3. Grid Side Converter. The GSC in Figure 6 usually governs the voltage at the DC link capacitor in turn controlling the active and reactive power. A vector control scheme is adopted here which maneuvers the grid parameters such that the voltage at DC link between the two converters remains constant. The grid parameters are observed and translated to their equivalent dq values, which are then aligned with that of the grid values. The three-phase grid voltages serve as the reference for this alignment, which is accomplished with the use of a phase-locked loop. Once this is accomplished, the PI controller is fed with the d-axis and q-axis grid currents to obtain the reference value for the PWM controller for the generation of pulses to the converter. Since the rotor's active power must flow through the DC link, it helps in regulating the active power precisely.

3. Modeling of DVR

DVR is connected in series with the grid and injects a three-phase voltage at PCC to recover the deficit voltage during faults. DVR is a unit comprising a DC power source and an inverter with an injection transformer. The switching signals for the inverter are generated using the pulse width modulation technique. Thus, DVR compensates for the sag arising due to fault thus securing the grid as well the wind turbine from any potential damage. The governing equations of a DVR model are represented in (3) to (4) [23].

The total power delivered is

$$S_{DVR} = V_{inj}{}^{*} I_L, \quad (3)$$

$$V_{inj} = \sqrt{2}^{*}\left|V_L\right|, \quad (4)$$

where I_L = load current, V_{inj} = injected voltage, and V_L = load voltage.

3.1. Control Strategy of DVR. In the proposed method, two FLCs, each for direct and quadrature axis of voltage, are designated to control DVR with two input and one output function as shown in Figure 7. The voltage at the load varies when there occurs a fault at the grid. Hence, the load voltage when compared with the reference grid voltage will yield an error value. These error values in all the phases are taken as the inputs for the fuzzy controller. The primary input is the error voltage (eV_{dL}, eV_{qL}), which is derived as the difference between the rated voltage and the varying voltage at load during fault. The other input is the change in error voltage (ΔeV_{dL}, ΔeV_{qL}). The output is the control voltage (V_d, V_q) given as the reference voltage to the PWM controller of the inverter.

3.2. Fuzzy Logic Controller of DVR. Even though PI is a traditional controller, it does not work well in changing and noisy environments. Also, there are many cases where superfluous proportional action may lead to unsteady output and an excessive integral action may lead to overshoots. To overcome this, a fuzzy operated DVR is explored in this research paper in the wind energy system. Fuzzy logic control (FLC) is a control system in which the net output depends on the state of the input and the corresponding change in the state of the input. Hence, fuzzy control yields more precise voltage restoration as close to that of nominal values, unlike a PI controller. As per the proposed method in this paper, two FLCs are used. One FLC is for the d-axis of the stator voltage and the other FLC is for the q-axis of the stator voltage each with two numbers of input membership functions (MFs) which are the error voltage and change in error voltage.

3.2.1. Membership Functions. In both FLCs, eight variables are assigned for the MF error and three variables are assigned for MF change in error respectively. The output MF has thirteen linguistic variables. Figures 8–10 illustrate the MFs of the input and output which are normalized between the values 1 and −1. The rules followed by the MFs are furnished in Table 3.

The rule viewer for FLC is shown in Figures 11 and 12 where error voltages are denoted by V_d and V_q respectively and changes in error voltages are denoted by DelV_d and DelV_q respectively. $V_d{}^{*}$ and $V_q{}^{*}$ are the outputs of the two FLCs each for the direct axis and the quadrature axis.

4. Electric Vehicle Charging Station

A vehicle-to-grid unit as shown in Figure 13 integrates the EV charging station to that of the grid. During the event of a fault, the wind system should stay connected to the grid as per the grid codes. Within this short duration, the voltage sag due to fault should be compensated instantly to avoid the disconnection of the wind source. Hence, the battery of the EV charging station provides compensation about the voltage sag intensity. The DC voltage of the battery is fed to an inverter of appropriate ratings. The output of the inverter is connected to the grid so that the voltage compensation takes place effectively and rapidly when a fault occurs.

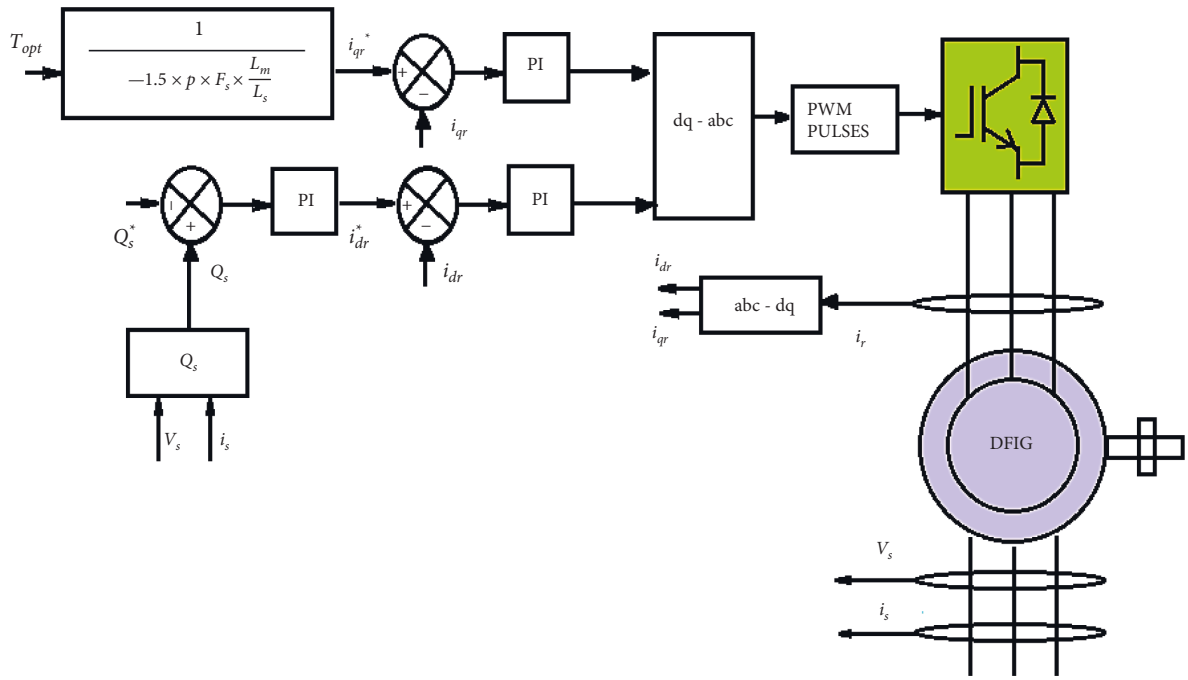

Figure 5: Rotor side converter.

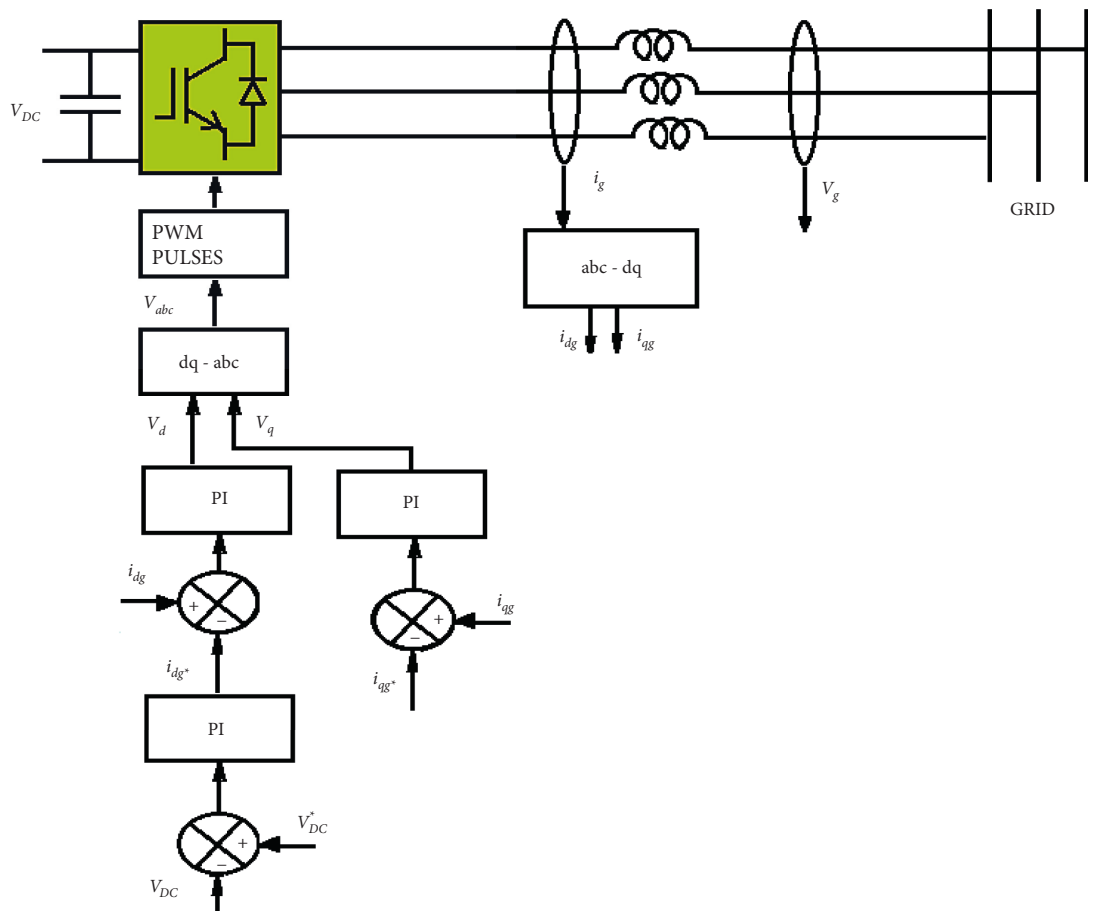

Figure 6: Grid side converter.

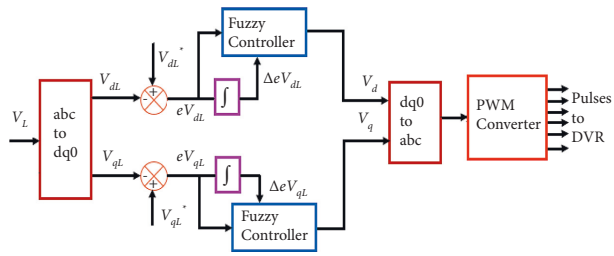

Figure 7: The fuzzy control diagram of DVR.

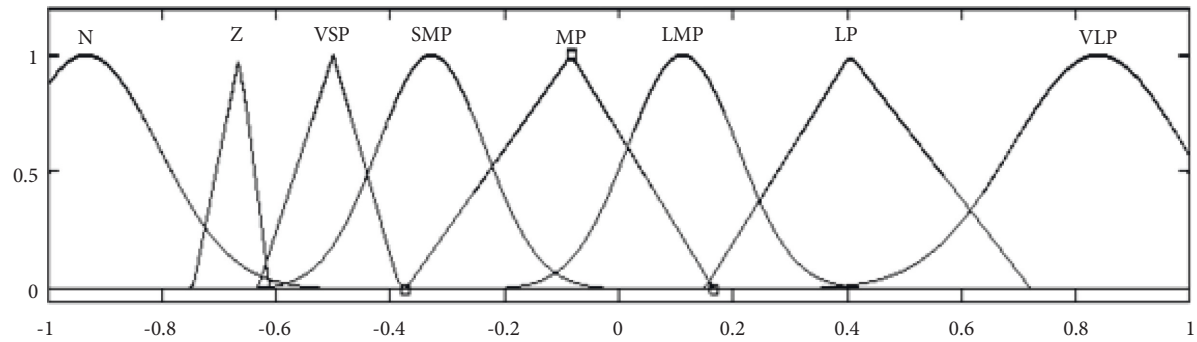

Figure 8: eV_{dL} and eV_{qL}—input MF.

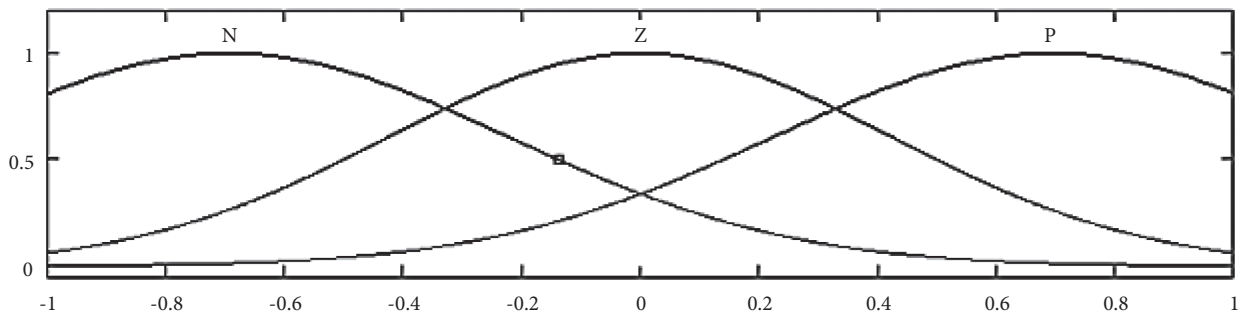

Figure 9: ΔeV_{dL} and ΔeV_{qL}—input MF.

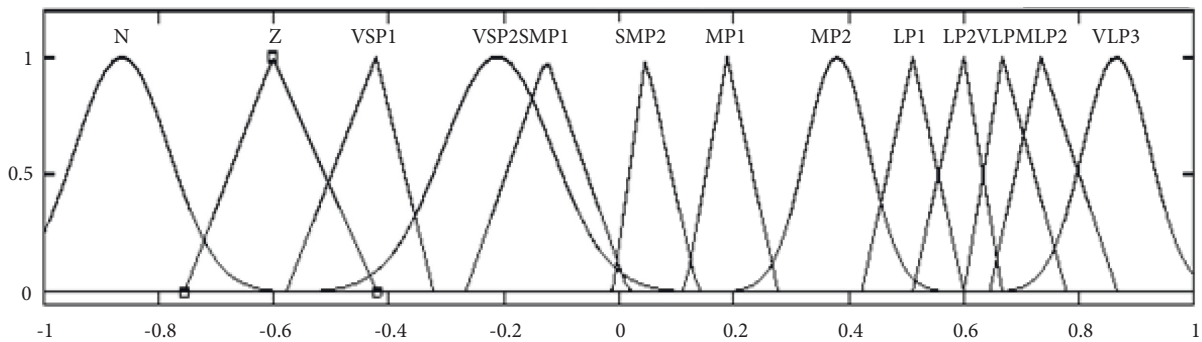

Figure 10: V_d and V_q—output MF.

Table 3: Rule base for FLC of DVR.

ΔeV_L	eV_L							
	VLP	LP	LMP	MP	SMP	VSP	Z	N
P	VLP3	VLP2	LP2	MP2	SMP2	VSP2	Z	N
Z	VLP3	VLP1	LP1	MP1	SMP1	VSP1	Z	N
N	VLP3	VLP1	LP1	MP1	SMP1	VSP1	Z	N

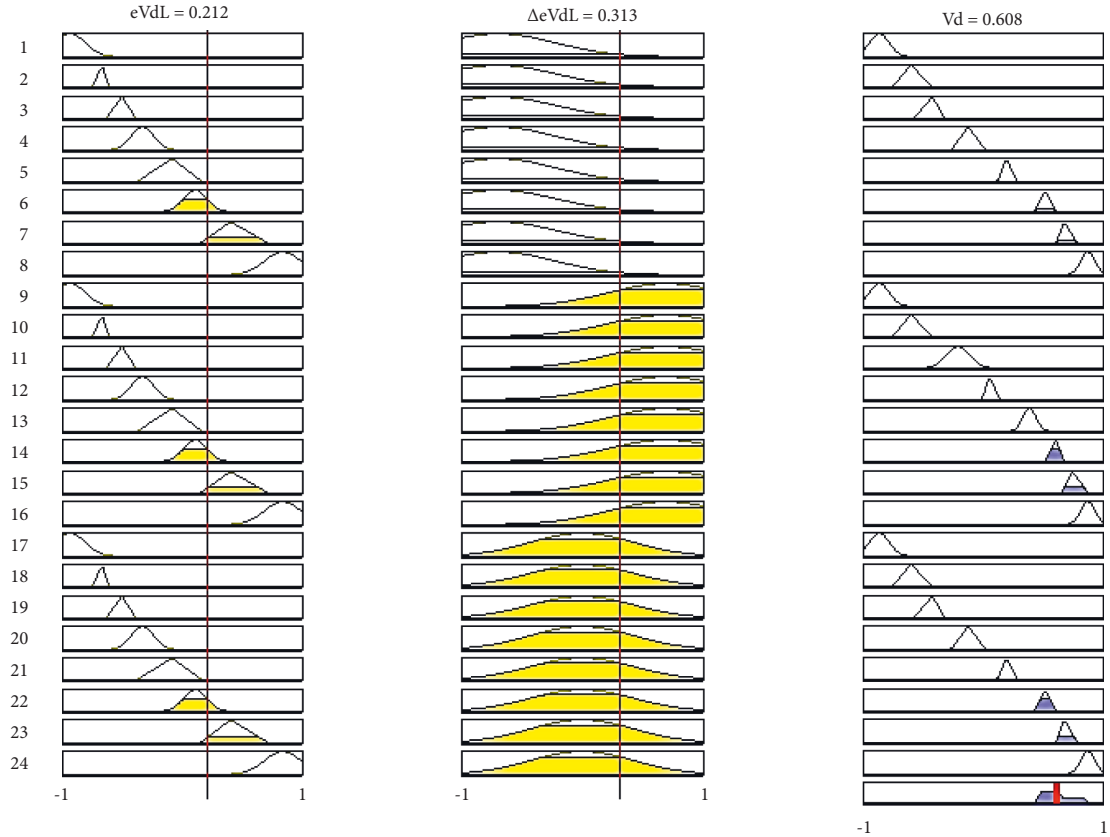

Figure 11: Rule viewer for V_d.

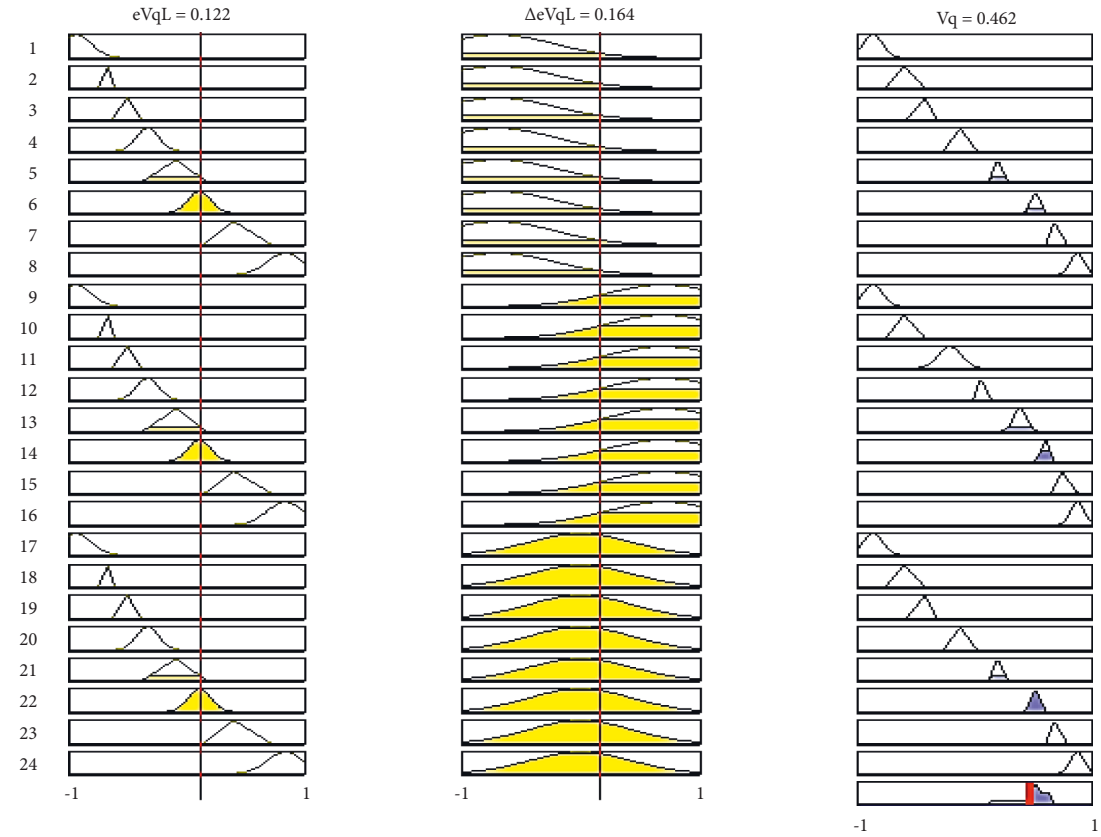

Figure 12: Rule viewer for V_q.

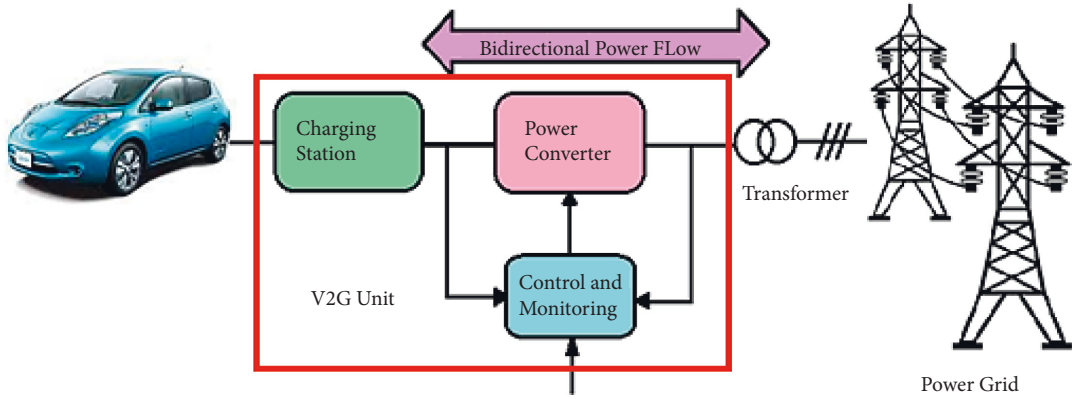

Figure 13: Voltage compensation with V2G unit.

4.1. EV Charging Station Structure. The EV charging station structure shown in Figure 14 is mainly powered by a PV source and includes bidirectional converters in which the energy can flow in both directions of the converter. A bidirectional converter regulates the voltage by regulating the duty cycle of the PWM controller with a certain frequency and duty ratio. By the variation of firing pulses, the buck and boost mode of the bidirectional converter charges and discharges the battery in the EV charging station depending on the necessity. The voltage during the battery discharge is conditioned and tied to the grid to supplement the voltage sag due to fault. The control unit of the charging station uses a P&O MPPT controller to retrieve maximum power from the PV source and generates a duty cycle for the PWM generator of the DC-DC converter. The pulses for the bidirectional converter are controlled and regulated by a fuzzy controller. The EV charging station is energized by a PV source whose parameters are listed in Table 4. An MPPT controller extracts maximum power from the source and it is fed to a boost converter as indicated in Figure 15. The output from the boost converter is fed to a bidirectional inverter for charging the battery. The bidirectional converter charges or discharges alternately depending on its pulses. These pulses are controlled using a fuzzy controller. The fuzzy controller has two input membership (V_d, SoC) functions and one output membership function (I). The output of the fuzzy controller along with its reference voltage variables is fed to a PI controller which generates pulses for the bidirectional converter based on (5). The complement of (5) yields pulses for discharging conditions.

$$\mathbf{V} = \mathbf{V_d} + \mathbf{k_p}\left(\mathbf{I_{batt}} - \mathbf{I^*_{batt}}\right) + \mathbf{k_i}\int\left(\mathbf{I_{batt}} - \mathbf{I^*_{batt}}\right)\mathbf{dt}, \quad (5)$$

where V = reference voltage for PWM controller for charging condition, V_d = DC-DC converter voltage, V, I^*_{batt} = reference current, I_{batt} = battery current, k_p = proportional constant of the PI controller, and ki = integral constant of the PI controller.

4.1.1. Membership Functions. The MFs have five linguistic variables as shown in Figure 15. The rules for the FLC are depicted in Table 5. The voltage from the DC/DC converter (V_d) and State of Charge (SoC) of the battery are intercepted as the inputs to the FLC and the current is intercepted as the output of the FLC.

5. Modes of Operation

5.1. Normal Mode. In this mode of operation as indicated in Figure 16, the power produced from the WECS is integrated with the grid. The DFIG-based wind system generates AC voltage which is converted to DC using RSC. The converted voltage is stored in the DC link capacitor. The DC link voltage is converted to AC via an inverter. The inverted AC output is integrated with the grid. In an EV charging station, the battery is charged by a separate PV source and continues to charge electric vehicles and the DVR stays idle in this mode of operation. Even though the output from the EV charging station and DVR is bound to the grid, in this operating mode the charging station or the DVR does not impact the grid integrated hybrid system. When the wind system encounters the fault, the charging station or the DVR takes over immediately pertaining to the intensity of the voltage sag thereby supplementing the shortfall voltage that is developed due to the fault.

5.2. Fault-Ride-Through Mode. This mode of operation is called FRT as a fault inculcated at PCC. During the event of a fault, the wind system should stay connected to the grid as

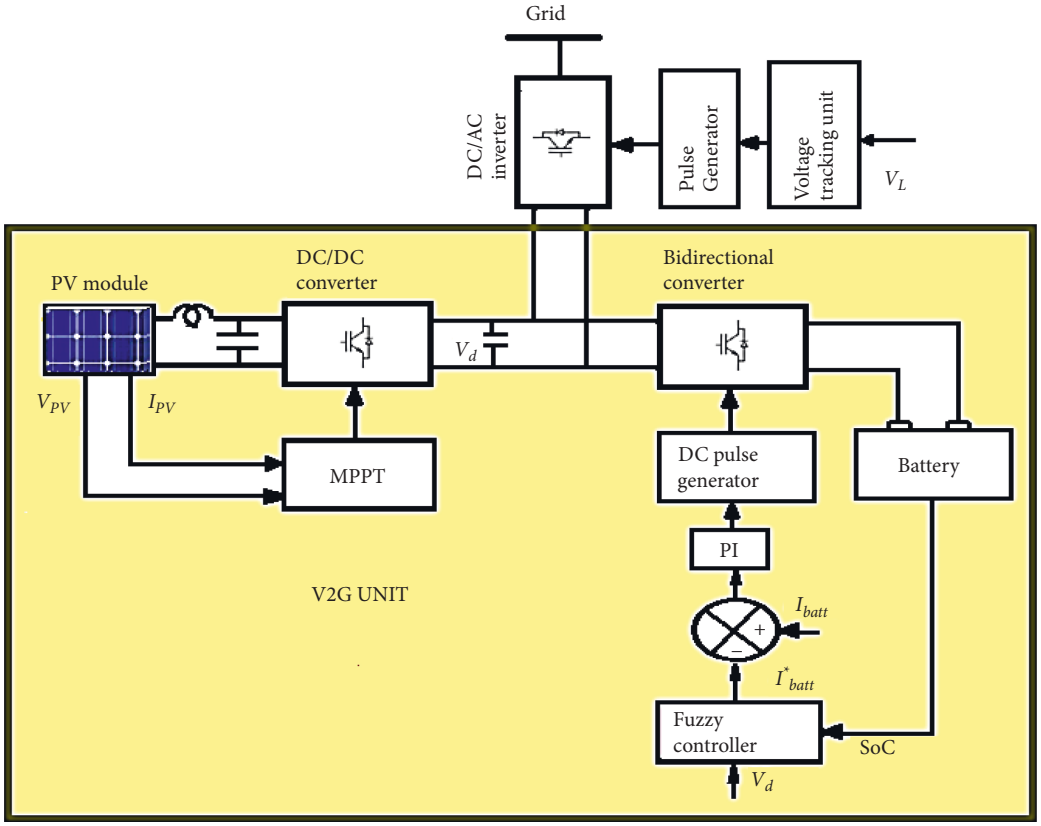

Figure 14: EV charging station.

Table 4: Electric vehicle design parameters.

Parameters	Value
DC-DC converter	
L	5 mH
C	100 μF
Bidirectional converter	
L	0.5 mH
C	1 mF

per the grid codes indicated in Figure 1. Within this short duration, the voltage sag due to fault should be compensated instantly to avoid the disconnection of the wind source. Hence, in this mode either the battery of the EV charging station discharges or the voltage is supplied by DVR, thereby compensating the deficit voltage about the intensity of the sag. The power flow for this mode of operation is shown in Figure 17. The V2G unit and the DVR are controlled using a switch about the intensity of the voltage sag. If voltage sag falls between 0.9 p.u. and 0.51 p.u., the EV charging station provides voltage from the battery which is fed to an inverter of appropriate ratings. The output of the inverter is connected to the grid so that the voltage compensation takes place effectively and rapidly when a fault occurs. For voltage sag falling between 0.5 p.u. and 0.2 p.u., the DVR dominates in providing voltage compensation.

6. Discussion of Simulation Results

A2.5 MW capacity WECS connected to the grid with DVR was taken as a test system and was simulated. The system data of the test system are furnished in Tables 6 and 7, respectively. Figures 18(a) and 18(b) portray the wind curve of the wind energy system and PV curves of the EV charger system. The design specifications of the EV charging station are listed in Tables 4 and 8.

6.1. Low Voltage Ride Through. LVRT has been tested for a voltage sag occurring due to various faults such as three-, two-, and single-phase faults. Figure 19(a) indicates a three-phase fault at the grid and the voltage compensation using DVR and EV charging stations depending on voltage sag intensity is indicated in Figures 19(b)–19(d), respectively. In all three cases of fault as it can be observed, the voltage compensation is provided by the DVR or V2G unit depending on the intensity of voltage sag.

Two-phase fault (Phase A and Phase B) is indicated in Figure 20(a) with its voltage compensation using DVR and EV charging station shown in Figures 20(b)–20(d). Phases A and B are exclusively provided with the compensation. Figure 20(b) depicts the injected voltage using DVR and Figure 20(c) indicates EV compensated voltage.

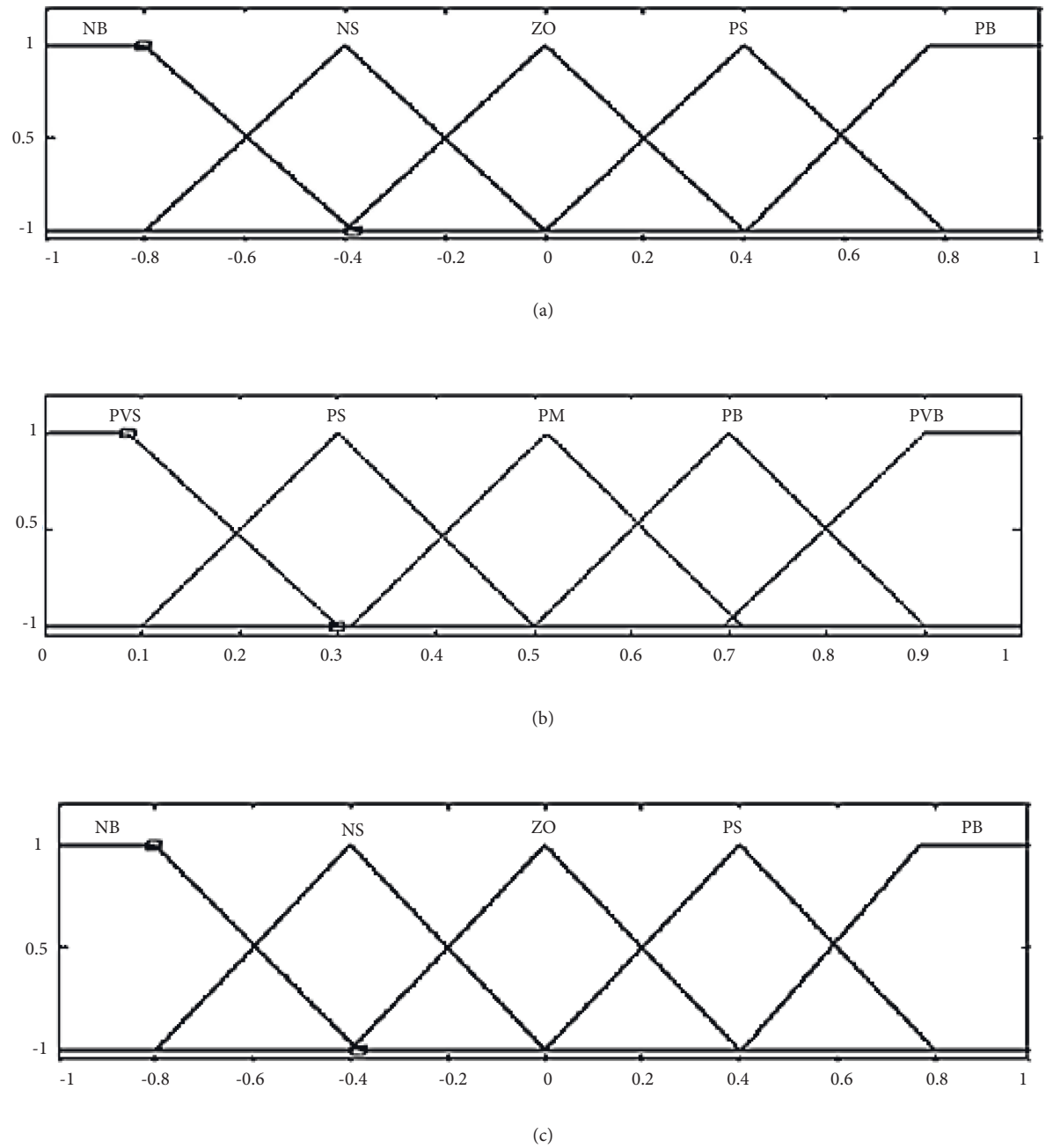

Figure 15: (a) V_d—input MF. (b) SoC—input MF. (c) I—output MF.

Table 5: Rules for FLC of EV charging station.

V_d	SoC				
	PVB	PB	PM	PS	PVS
PB	PB	NB	NB	PB	PB
PS	PB	NS	NS	PS	PS
ZO	PB	PS	ZO	ZO	ZO
NS	PB	PS	PS	PB	PB
NB	PB	PB	PB	PB	PB

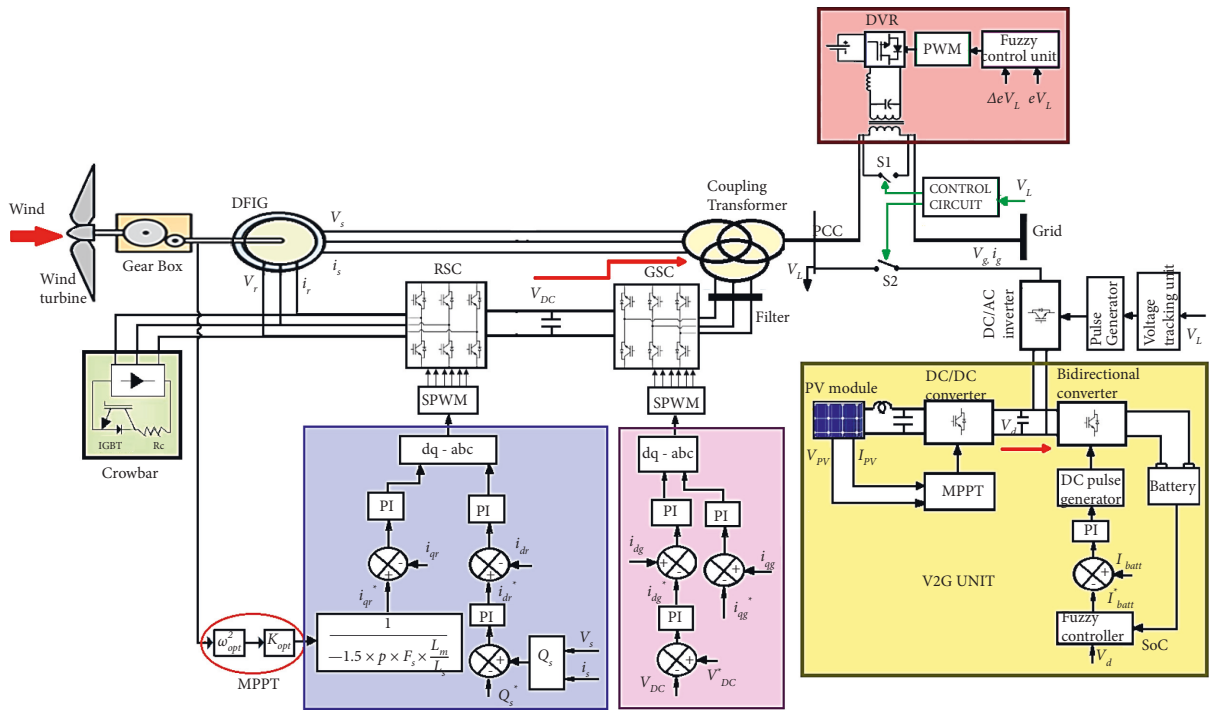

Figure 16: Normal mode of operation.

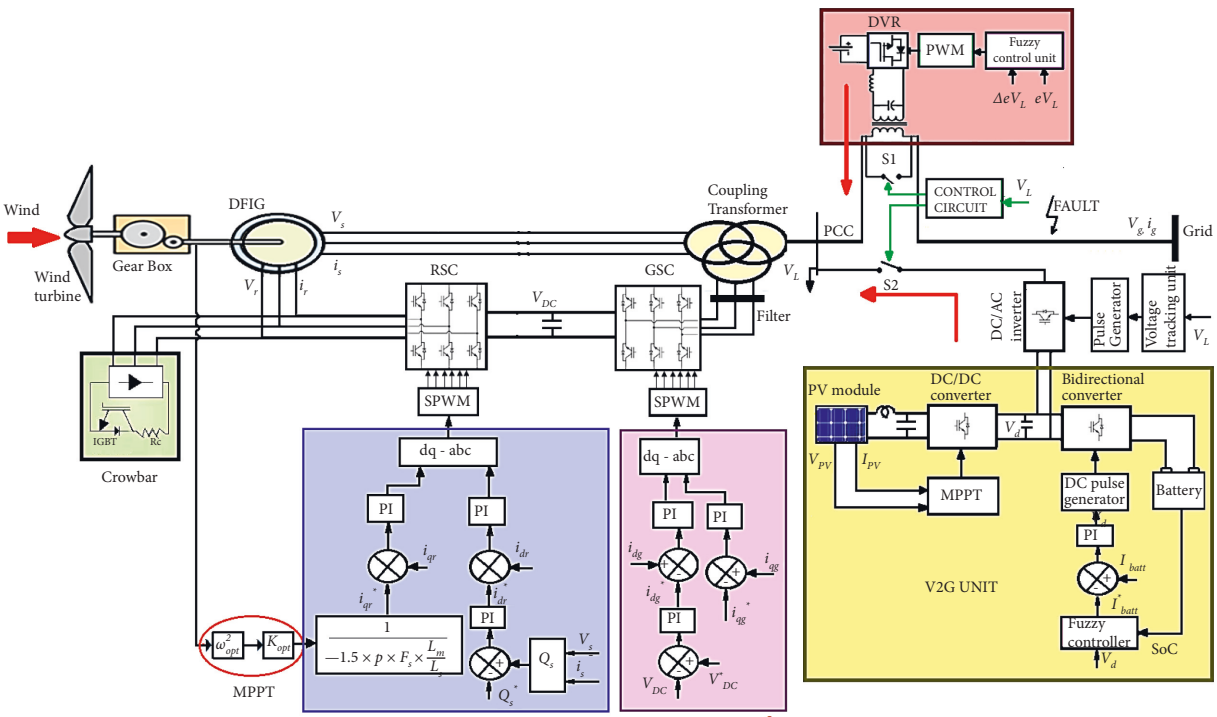

Figure 17: Fault ride Through Mode.

Table 6: DFIG machine ratings.

DFIG characteristics	Value
Power	2.5 MW
Stator voltage	690 V
Stator current	1760 A
Frequency	50 Hz
Stator connection	Star
Rotor connection	Star
Poles	2
R_s	$2.6e-3\ \Omega$
L_s	$0.087e-3$ H
L_m	$2.5e-3$ H
R_r	$2.9e-3\ \Omega$

Table 7: DVR ratings.

DVR parameters	Value
Power	2.5 MVA
L	0.1 mH
C	1 μF
Switching frequency	1000 Hz

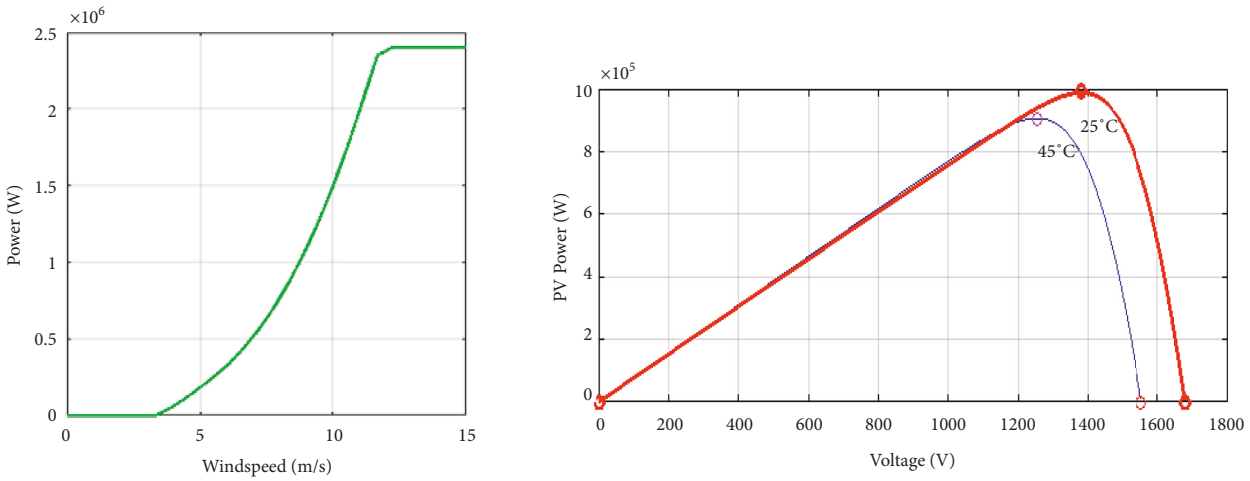

Figure 18: (a) Wind power curve and (b) PV curve.

Table 8: PV parameters of EV charging station.

PV parameters	Value
Power	1 MW
V_{oc}	37.3 V
I_{sc}	8.66 A
V_{mp}	30.7 V
I_{mp}	8.15 A
Cells per module	60
Parallel strings	88
Series strings	45

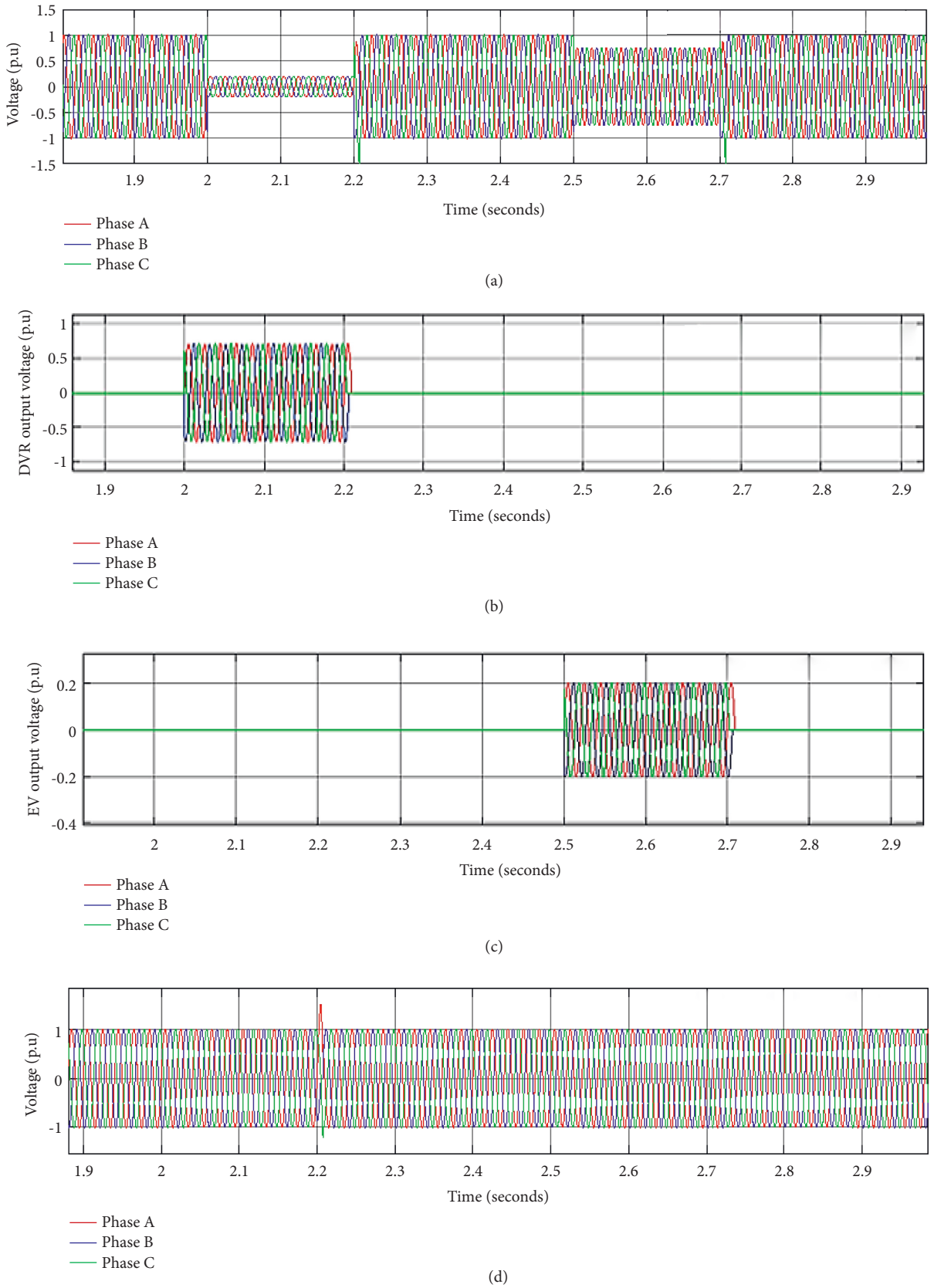

Figure 19: Three-phase fault. (a) Fault voltage. (b) Injected voltage using DVR. (c) Injected voltage using EV. (d) Voltage compensation.

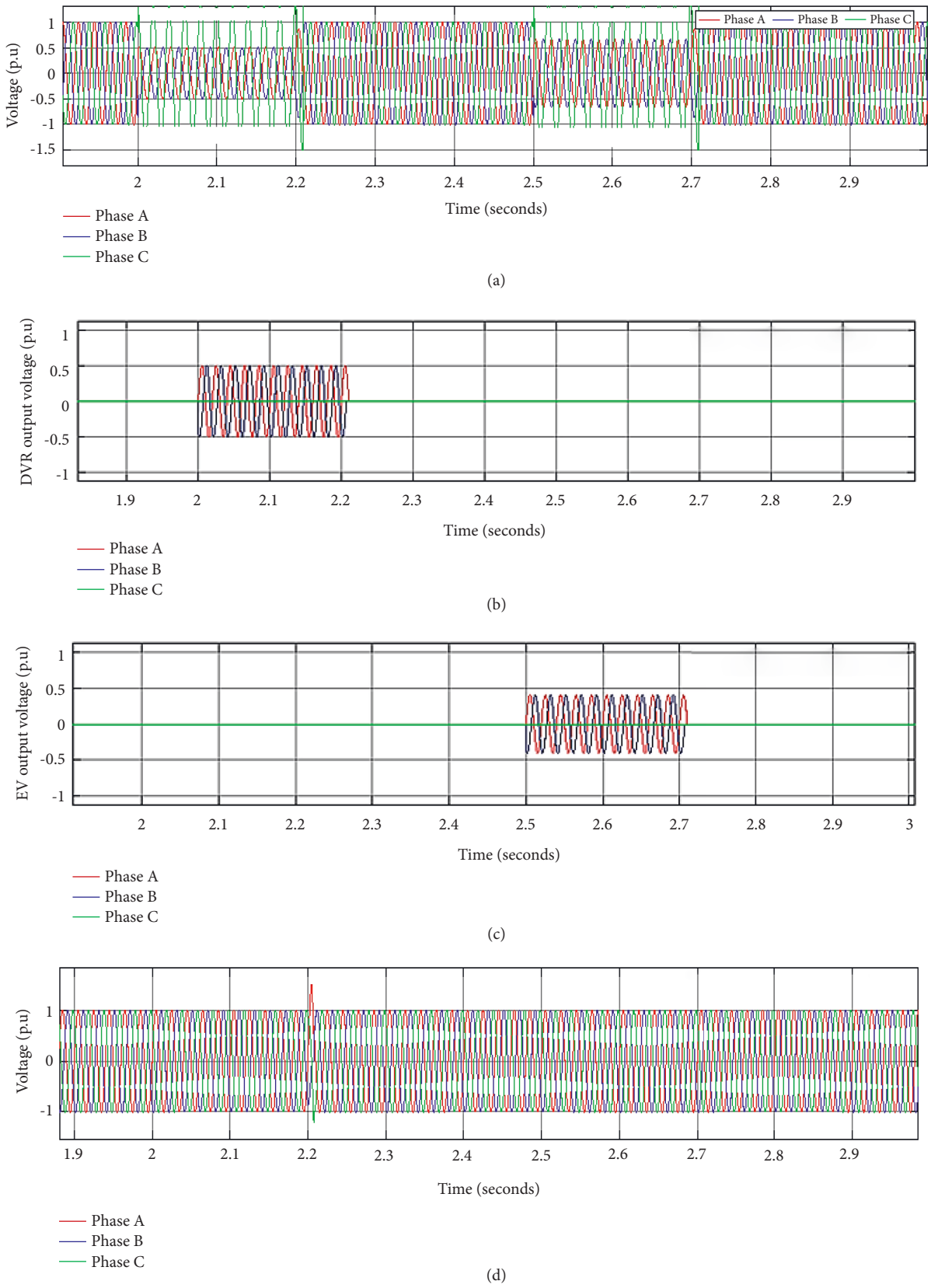

Figure 20: Two-phase fault. (a) Fault voltage in Phases B and C. (b) Injected voltage using DVR. (c) Injected voltage using EV. (d) Voltage compensation.

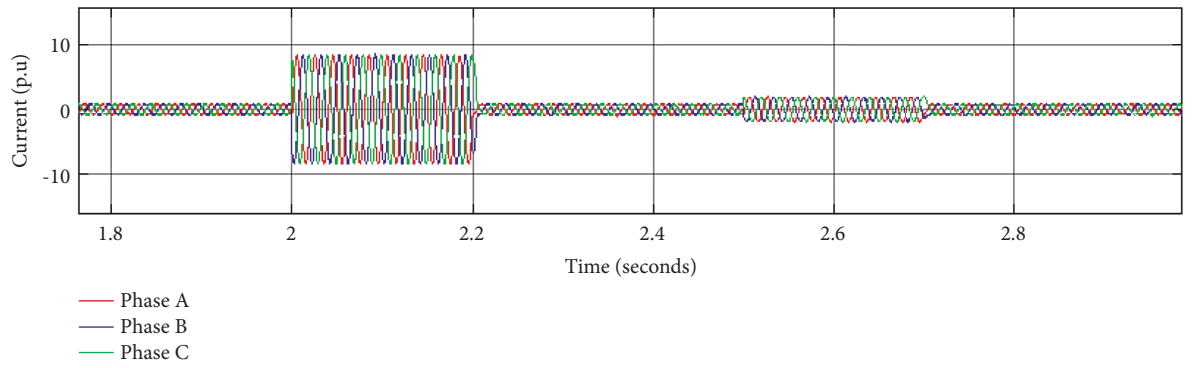

(a)

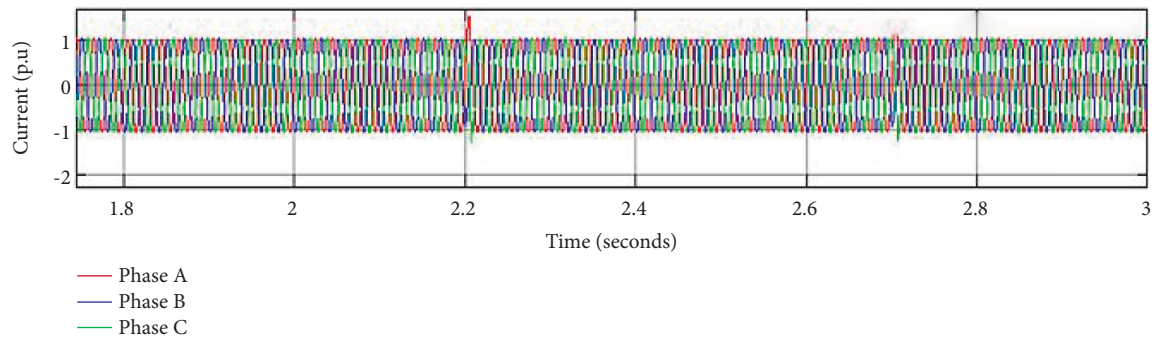

(b)

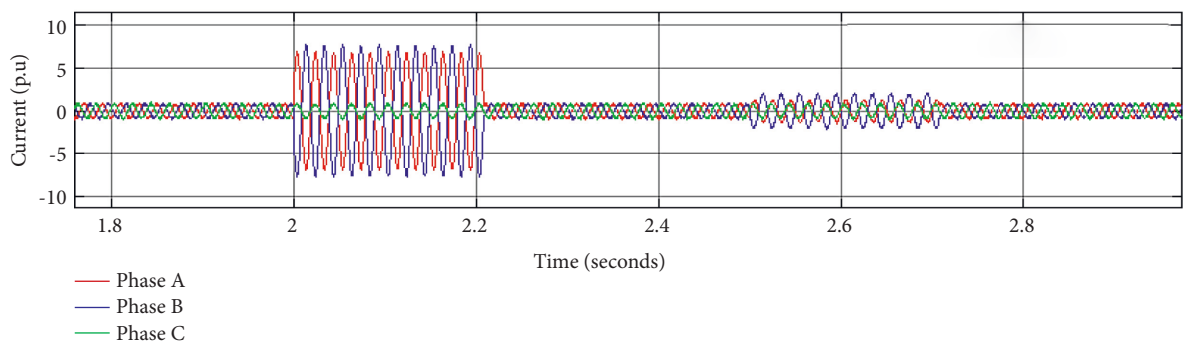

(c)

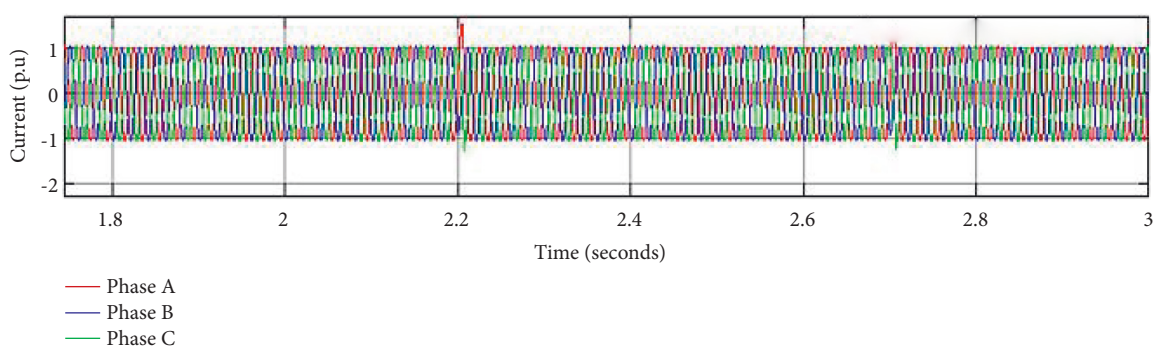

(d)

Figure 21: Continued.

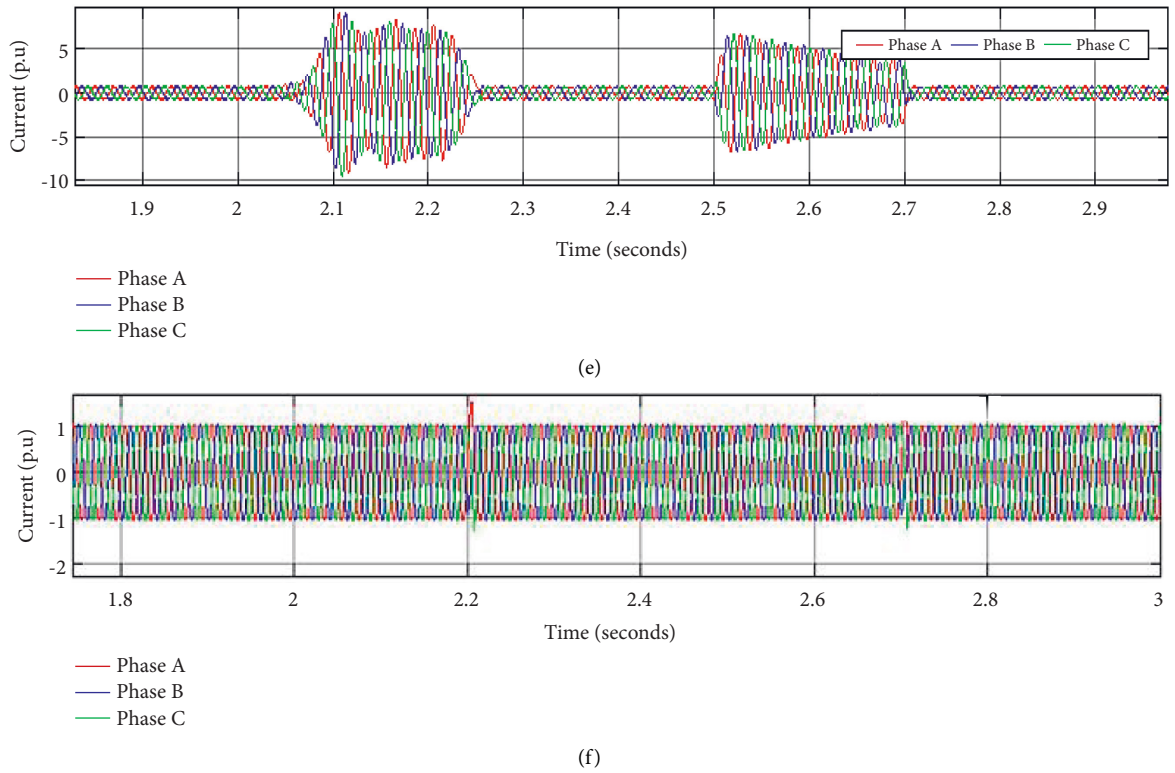

Figure 21: (a) Three-phase fault current. (b) Three-phase compensated current. (c) Two-phase fault current. (d) Two-phase compensated current. (e) Single-phase fault current. (f) Single-phase compensated current.

Likewise, the single-phase fault and its compensation are illustrated in Figure 21. Figures 22(a)–22(c) show single-phase fault (Phase A) along with its compensation using DVR and EV charging station. Figure 22(d) shows the net compensated voltage together with the DVR and EV charging station.

The stator current output for different faults is shown in Figure 21. When a fault occurs, due to the resulting voltage sag in the faulty phases, there is a sharp rise in current to a very high value which is shown in Figures 21(a), 21(c), and 21(e) for three-, two-, and single-phase faults successively. When DVR and EV charging stations offer voltage compensation, the restoration should include the current to fall back to its nominal range as well. This is achieved as shown in Figures 21(b), 21(d), and 21(f), respectively, for three-, two-, and single-phase fault.

The DC link voltage is an important parameter in providing a constant voltage to the grid. Whenever a fault occurs, owing to its accompanying voltage sag, there is an immediate drop in DC link voltage. One of the other jobs of any voltage compensation network is to retain a steady DC link voltage and active power. DVR and V2G compensation as can be seen in Figure 23 shifts the sudden drop in the DC link voltage and brings it to the nominal value. The regulation of DC voltage concerning both PI and fuzzy controller for V2G and DVR compensation is indicated in Figure 24. The fuzzy controller provides better stabilization of DC link voltage as compared to the PI controller in maintaining the constant DC link voltage during the different intensities of faults at 2 and 2.5 seconds respectively.

The power curve in Figure 24 highlights the DVR compensation and V2G compensation both wielding fuzzy control, thereby providing excellent compensation in maintaining constant active power at PCC.

6.2. DVR Output Voltage. Table 9 encapsulates the DVR voltage compensation between 2 and 2.2 seconds for different faults in p.u. values for PI and fuzzy controller. With three-phase faults, there is a uniform dip in all the three-phase voltages. It can be seen that with fuzzy controlled DVR, the voltage recovered is close to the nominal value for all the faults when compared to PI control.

6.3. EV Battery Charging and Discharging. The battery in the EV charging station will continue to charge from its PV source during the normal operation of the hybrid system. When a fault occurs, the battery automatically discharges to the grid to supplement the deficit of voltage occurring due to voltage sag. Figure 25 indicates the battery SoC when a fault occurs between the instant 2.5 and 2.7 seconds with PI and FLC. It can be seen that the battery begins to discharge at

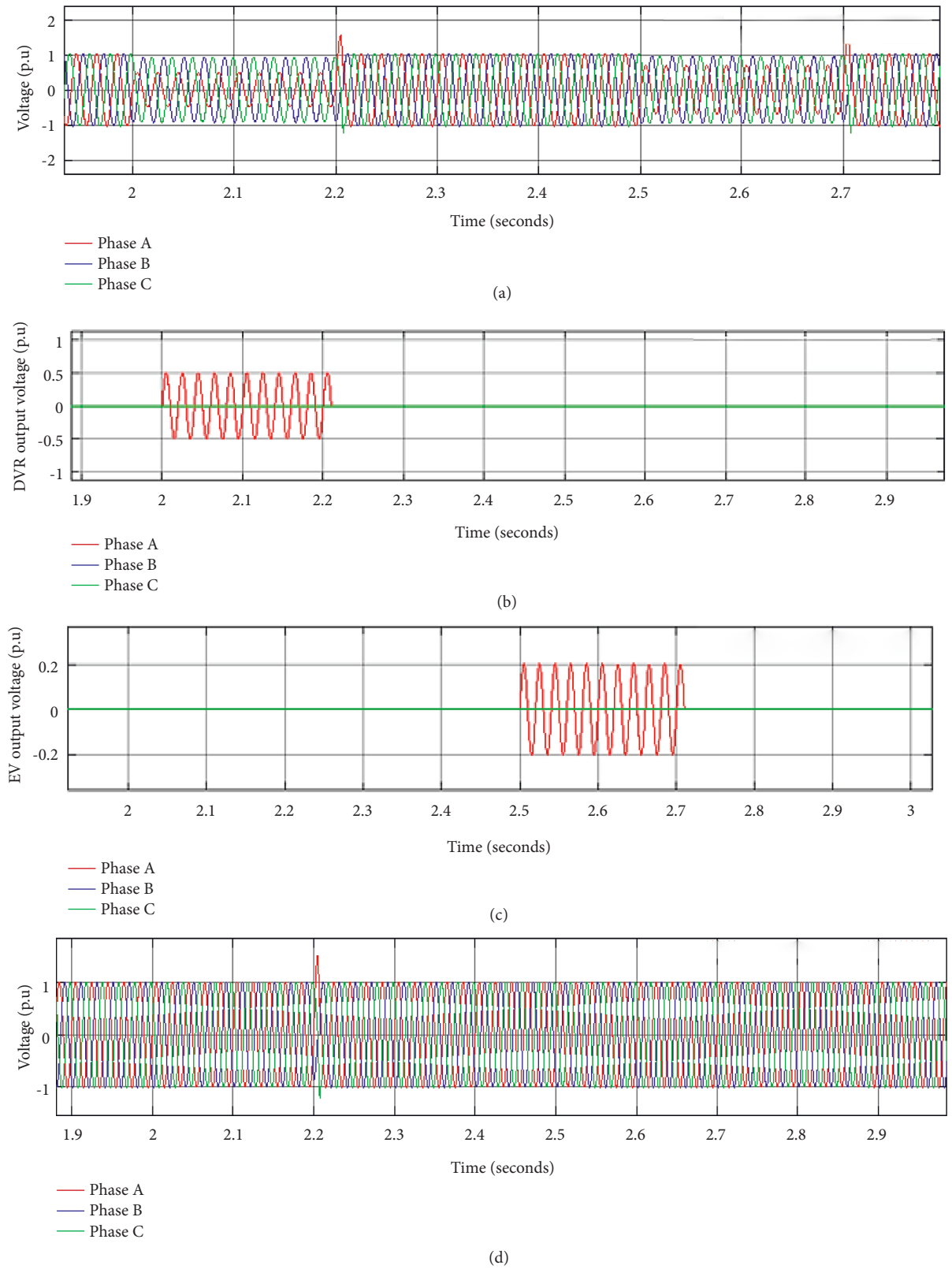

FIGURE 22: (a) Voltage during single-phase fault (Phase A). (b) Injected voltage using DVR. (c) Injected voltage using EV. (d) Voltage compensation for single-phase fault.

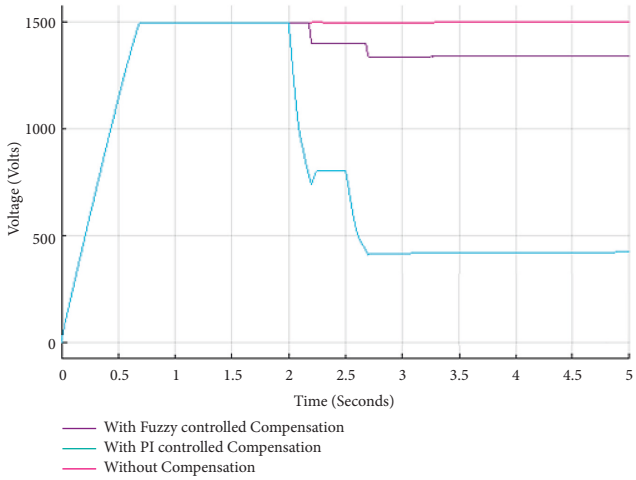

Figure 23: DC link voltage.

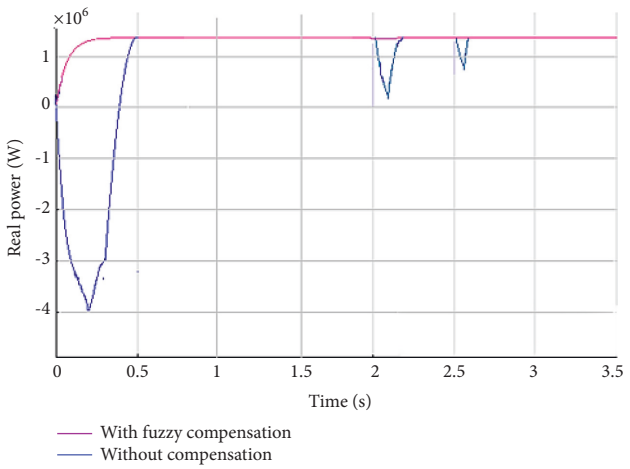

Figure 24: Active power for a wind speed of 9 m/s.

Table 9: DVR compensated voltage with PI and fuzzy control.

DVR controller	Fault voltage in p.u.			Compensated voltage in p.u.		
	Phase A	Phase B	Phase C	Phase A	Phase B	Phase C
Three-phase fault						
PI	0.3602	0.3613	0.3504	0.9564	1.184	0.9793
Fuzzy	0.3601	0.3614	0.3505	1.055	1.015	1.021
Two-phase fault						
PI	1.02	0.3862	0.3265	1.02	1.169	1.088
Fuzzy	1.02	0.3864	0.3266	1.02	1.028	1.023
Single-phase fault						
PI	1.027	1.012	0.3105	1.029	1.012	0.8846
Fuzzy	1.027	1.012	0.3103	1.021	1.01	1.044

exactly the instant of 2.5 seconds. At exactly 2.7 seconds, the battery with fuzzy control again resumes charging as the fault period with less intensity is only between 2.5 and 2.7 seconds. But, with the PI controller, the charging resumes only after 2.8 seconds as indicated in Figure 25. Hence, fuzzy

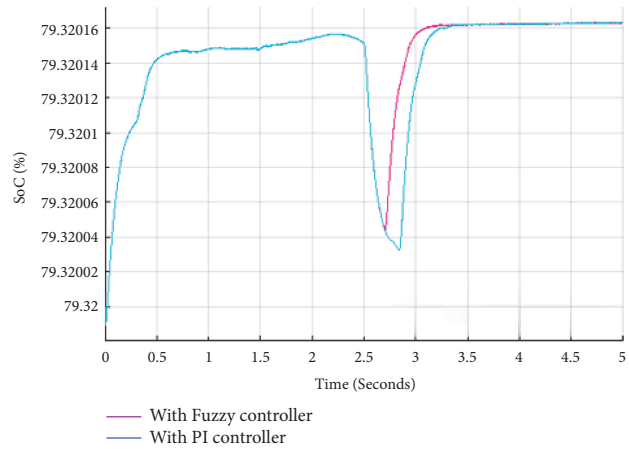

Figure 25: V2G compensation voltage for 3 phases.

control provides more precise control in balancing the charging and discharging period than PI control.

7. Conclusion

This paper explores the effectiveness of DVR and V2G integrated system-based voltage compensation for the FRT capability of DFIG fed wind energy systems. DVR connected in series with the stator voltage is considered to be a more effective compensation technique for the stator voltage when the voltage sag intensity falls between 0.5 p.u. and 0.2 p.u. during various faults such as three-, two-, and single-phase faults. Similarly, the V2G system comes into action when the voltage sag intensity falls between 0.9 p.u. and 0.51 p.u. The voltage restored reaches the original stator voltage as soon as DVR or the V2G system is switched on. The voltage across the DC link capacitor falls to a low value without any compensation which is also brought to its original value with the compensation. The results showed clearly that employing fuzzy control for both supplementary devices yields a better control than a PI controller. Similarly, the change inactive power due to voltage sag is found to be balanced out with both DVR and V2G units clearly for all the faulty conditions. Thus, the DVR/V2G system is found to give reliable compensation and FRT is achieved during the period of fault.

Nomenclature

EV: Electric vehicle
WECS: Wind energy conversion system
DFIG: Doubly fed induction generator
FRT: Fault ride through
DVR: Dynamic voltage restorer
V2G: Vehicle to grid
PCC: Point of common coupling
RSC: Rotor side converter
GSC: Grid side converter
FLC: Fuzzy logic controller
MF: Membership function
FAME:

Faster adoption and manufacturing of electric vehicles.

Data Availability

No data were used to support this study.

Conflicts of Interest

The authors declare that they have no conflicts of interest.

Authors' Contributions

All authors have contributed equally.

References

[1] S. Worldwide, Number of Electric Cars, 2020, online: https://www.statista.com/study/11578/electric-vehicles-statistadossier.

[2] *Data from Society of Manufacturers of Electric Vehicles*, 2020.

[3] *Indian Electricity Grid Code*, Central Electricity Regulatory Commission, New Delhi, India, 2010.

[4] N. Khatoon and S. Shaik, "Review of different fault ride through control strategies for a DFIG wind turbine," *International Research Journal of Engineering and Technology*, vol. 4, 2017.

[5] M. Mohseni and S. M. Islam, "Review of international grid codes for wind power integration: diversity, technology and a case for global standard," *Renewable and Sustainable Energy Reviews*, vol. 16, 2012.

[6] A. Nduwamungu, E. Ntagwirumugara, F. Mulolani, and W. Bashir, "Fault ride through capability analysis in wind power plants with doubly fed induction generators for smart grid technologies," *Energies*, vol. 13, 2020.

[7] M. Mohseni and S. M. Islam, "Transient control of DFIG-based wind power plants in compliance with the Australian grid code," *IEEE Transactions in Power Electronics*, vol. 27, 2012.

[8] Z. Yang and Y. Chai, "A survey of fault diagnosis for onshore grid-connected converter in wind energy conversion systems," *Renewable and Sustainable Energy Reviews*, vol. 66, 2016.

[9] B. Jain and S. J. R. K. Nema, "Control strategies of grid interfaced wind energy conversion system: an overview," *Renewable and Sustainable Energy Reviews*, vol. 47, 2015.

[10] M. Javad Morshed and A. Fekih, "A new fault ride-through control for DFIG-based wind energy systems," *Electric Power Systems Research*, vol. 146, 2017.

[11] M. R. Amer and O. A. Mahgoub, "New switching technique for current control of grid converters for wind power systems," *Sustainable Energy, Grids and Networks*, vol. 9, 2017.

[12] G. Sarwar Kaloi, J. Wang, and M. Hussain Baloch, "Active and reactive power control of the doubly fed induction generator based on wind energy conversion system," *Energy Reports*, vol. 2, 2016.

[13] H. Sardar Kamil, D. Mat Said, M. Wazir Mustafa, M. Reza Miveh, and N. Ahmad, "Low-voltage ride-through methods for grid-connected photovoltaic systems in microgrids: a review and future prospect," *International Journal of Power Electronics and Drive Systems (IJPEDS)*, vol. 9, no. 4, p. 1834, 2018.

[14] M. Shuaibu, A. S. Abubakar, and A. F. Shehu, "Techniques for ensuring fault ride-through capability of grid connected DFIG-based wind turbine systems: a review," *Nigerian Journal of Technological Development*, vol. 18, no. 1, pp. 39–46, 2021.

[15] H. Geng, C. Liu, and G. Yang, "LVRT capability of DFIG-based WECS under asymmetrical grid fault condition," *IEEE Transactions on Industrial Electronics*, vol. 60, no. 6, pp. 2495–2509, 2013.

[16] J. Yao, H. Li, Z. Chen et al., "Enhanced control of a DFIG-based wind-power generation system with series grid-side converter under unbalanced grid voltage conditions," *IEEE Transactions on Power Electronics*, vol. 28, no. 7, pp. 3167–3181, 2013.

[17] G. Angala Parameswari and H. Habeebullah Sait, "A comprehensive review of fault ride-through capability of wind turbines with grid-connected doubly fed induction generator," *International Transactions of Electrical Energy Systems*, vol. 30, 2020.

[18] O. Noureldeen and I. Hamdan, "A novel controllable crowbar based on fault type protection technique for DFIG wind energy conversion system using adaptive neuro-fuzzy inference system," *Protection and Control of Modern Power Systems*, vol. 3, no. 1, p. 35, 2018.

[19] N. Omar and I. Hamdan, "Design of robust intelligent protection technique for large-scale grid-connected wind farm"," *Journal of Protection and Control of Modern Power Systems*, vol. 3, no. 17, pp. 1–13, 2018.

[20] M. K. Dösoglu, A. B. Arsoy, and U. Güvenç, "Application of STATCOM-supercapacitor for low-voltage ride-through capability in DFIG-based wind farm," *Neural Computing Applications*, vol. 28, 2016.

[21] R. Hiremath and T. Moger, "Comprehensive review on low voltage ride through capability of wind turbine generators," *International Journal of Electrical Energy Systems*, vol. 30, 2020.

[22] H. Rezaie and M. H. Kazemi-Rahbar, "Enhancing voltage stability and LVRT capability of a wind-integrated power system using a fuzzy-based SVC," *Engineering Science and Technology, an International Journal*, vol. 22, no. 3, pp. 827–839, 2019.

[23] A. O. Ibrahim, T. H. Nguyen, and D.-C. Lee, "A fault ride-through technique of DFIG wind turbine systems using dynamic voltage restorers," *IEEE Transactions on Energy Conversion*, vol. 26, 2011.

[24] R. A. J. Amalorpavaraj, P. Kaliannan, S. Padmanaban, U. Subramaniam, and V. K. Ramachandaramurthy, "Improved fault ride through capability in DFIG based wind turbines using dynamic voltage restorer with combined feed-forward and feed-back control," *IEEE Access*, vol. 5, 2017.

[25] G. Sivasankar and V. S. Kumar, "Improving stability of utility-tied wind generators using dynamic voltage restorer," *Journal of Energy in Southern Africa*, vol. 25, no. 4, pp. 71–79, 2014.

[26] Y. He, M. Wang, and Z. Xu, "Coordinative low voltage ride through control for the wind-photovoltaic hybrid generation system," *IEEE Journal of Emerging and Elected Topics in Power Electronics*, vol. 8, 2020.

[27] P. Sathish Babu and N. Kamaraj, "Performance investigation of dynamic voltage restorer using PI and fuzzy controller," in *Proceedings of the International Conference on Power Energy and Control*, Dindigul, India, Febraury 2013.

[28] *Electric Vehicle Charging Infrastructure a Guide for Discom Readiness*, Rocky Mountain Institute Collaborative, New Delhi, India, 2020.

[29] F. Shaaban, A. A. Eajal, and E. F. El-Saadany, "Coordinated charging of plug-in hybrid electric vehicles in smart hybrid AC/DC distribution systems," *Renewable Energy*, vol. 82, 2014.

[30] Y. Ota, H. Taniguchi, T. Nakajima, K. M. Liyanage, J. Baba, and A. Yokoyama, "Autonomous distributed V2G

satisfyingscheduled charging," *IEEE Transactions on Smart Grid*, vol. 3, 2012.

[31] A. Mohammad, R. Zamora, and T. Tjing Lie, "Integration of electric vehicles in the distribution network: a review of PV based electric vehicle modelling," *Energies*, vol. 13, 2020.

[32] B. Morris, F. Foiadelli, C. Leone, and M. Longo, "Electric vehicles charging technology review and optimal size estimation," *Journal of Electrical Engineering & Technology*, vol. 15, 2020.

[33] F. De Luca, V. Calderaro, and V. Galdi, "A fuzzy logic-based control algorithm for the recharge/V2G of a nine-phase integrated on-board battery charger," *Electronics*, vol. 9, 2020.

[34] R. Uthra and D. Suchitra, "Fault ride through in grid integrated hybrid system using facts device and electric vehicle charging station," *Energies*, vol. 14, 2021.

[35] R. Uthra and D. Suchitra, "A fuzzy based improved control strategy of dynamic voltage restorer for low voltage and high voltage ride through compensation for variable speed hybrid energy system," *Wireless Personal Communications*, 2021.